



HAL
open science

Structural and microstructural characterization of $\text{CuMo}(1-x)\text{W}_x\text{O}_4$ ($x \leq 0.12$) ceramics sintered by spark plasma sintering

Mohamed Benchikhi, Rachida El Ouatib, Sophie Guillemet, Lahcen Er-Rakho, Bernard Durand

► **To cite this version:**

Mohamed Benchikhi, Rachida El Ouatib, Sophie Guillemet, Lahcen Er-Rakho, Bernard Durand. Structural and microstructural characterization of $\text{CuMo}(1-x)\text{W}_x\text{O}_4$ ($x \leq 0.12$) ceramics sintered by spark plasma sintering. Global Journal of Engineering Science and Research Management, 2015, 2 (12), pp.123-128. hal-02094693

HAL Id: hal-02094693

<https://hal.science/hal-02094693>

Submitted on 9 Apr 2019

HAL is a multi-disciplinary open access archive for the deposit and dissemination of scientific research documents, whether they are published or not. The documents may come from teaching and research institutions in France or abroad, or from public or private research centers.

L'archive ouverte pluridisciplinaire **HAL**, est destinée au dépôt et à la diffusion de documents scientifiques de niveau recherche, publiés ou non, émanant des établissements d'enseignement et de recherche français ou étrangers, des laboratoires publics ou privés.






Open Archive Toulouse Archive Ouverte (OATAO)

OATAO is an open access repository that collects the work of Toulouse researchers and makes it freely available over the web where possible

This is an author's version published in: <http://oatao.univ-toulouse.fr/23648>

Official URL: <http://www.gjesrm.com/Issues%20PDF/Archive-2015/December-2015/15.pdf>

To cite this version:

Benchikhi, Mohamed  and El Ouatib, Rachida and Guillemet, Sophie  and Er-Rakho, Lahcen and Durand, Bernard  *Structural and microstructural characterization of $\text{CuMo}(1-x)\text{WxO}_4$ ($x \leq 0.12$) ceramics sintered by spark plasma sintering.* (2015) *Global Journal of Engineering Science and Research Management*, 2 (12). 123-128. ISSN 2349-4506

Any correspondence concerning this service should be sent to the repository administrator: tech-oatao@listes-diff.inp-toulouse.fr

STRUCTURAL AND MICROSTRUCTURAL CHARACTERIZATION OF $\text{CuMo}_{(1-x)}\text{W}_x\text{O}_4$ ($x \leq 0.12$) CERAMICS SINTERED BY SPARK PLASMA SINTERING

M. Benchikhi^{1, 2}, R. El Ouati^{1*}, S. Guillemet-Fritsch², L. Er-Rakho¹, B. Durand²

¹Laboratoire de Physico-Chimie des Matériaux Inorganiques, Faculté des sciences Ain Chock, Hassan II University of Casablanca, B.P 5366 Maarif, Maroc.

²Institut Carnot CIRIMAT, CNRS Université de Toulouse, 118 route de Narbonne, 31062 Toulouse Cedex 9, France.

KEYWORDS: Spark plasma sintering (SPS), Chemical preparation, Structural phase transition, Molybdate, Tungsten.

ABSTRACT

Cupric molybdate CuMoO_4 is an interesting material due to their rich electrical, optical and magnetic properties. In this work, Solid solutions $\text{CuMo}_{(1-x)}\text{W}_x\text{O}_4$ ($x \leq 0.12$) were obtained by pyrolysis at 400 -700°C for 2 hours of a polymeric precursors elaborated by polymerizable complex method. For $x \leq 0.075$, they were isostructural with α - CuMoO_4 and for $0.075 < x \leq 0.12$, they were isostructural with γ - CuMoO_4 . Spark Plasma Sintering (SPS) at 300°C for 5 min under an applied pressure of 200 MPa led to variety CuMoO_4 -III for tungsten contents in the range 0.075-0.12.

INTRODUCTION

In recent years, transition metal molybdates AMoO_4 (with $A = \text{Cu}^{2+}, \text{Ni}^{2+}, \text{Co}^{2+}, \text{Fe}^{2+}$) have been largely studied owing to their theoretical and practical interests. Especially, copper molybdate CuMoO_4 has been studied extensively due to their excellent piezochromic, thermochromic and magnetic properties and their potential applications as oxidation catalysts in chemical and petrochemical processes [1-7]. Numerous authors have studied the temperature and pressure dependences of the optical, electrical and magnetic properties of CuMoO_4 [7-11].

Several polymorphs of CuMoO_4 have been reported in the literature [7,12], this depends on temperature and pressure as well as the synthesis conditions. The stable polymorph under standard conditions of temperature and pressure is triclinic α - CuMoO_4 (P1 space group) [7]. The γ - CuMoO_4 phase (also $P\bar{7}$) is stable below 200 K [7]. For temperatures above 840 K a polymorph of hexagonal symmetry, β - CuMoO_4 , has been reported [13]. Both polymorphs CuMoO_4 -II and CuMoO_4 -III are high-pressure modifications with wolframite type structure, but remain stable at ambient conditions. They are isostructural to CuWO_4 [14,15]. Furthermore the polymorph ε - CuMoO_4 has recently been reported [12]. Moreover, the temperatures/pressures of transition are adjustable by chemical doping [4,7]. CuMoO_4 -III, CuMoO_4 -II and ε - CuMoO_4 are antiferromagnetic at low temperatures whereas α - CuMoO_4 and γ - CuMoO_4 do not show any magnetic ordering until 2K [5,12,13,15].

Numerous synthesis procedures of the molybdate CuMoO_4 have been investigated: solid state reaction [13], mechano-synthesis [16], co-precipitation [17], pyrolysis [18], polyol method [19] and recently the polymerizable complex method [20,21]. This latter, allowing the control of the particles size, the composition and the homogeneity of powders [20-23], was chosen for the preparation of the solid solutions $\text{CuMo}_{(1-x)}\text{W}_x\text{O}_4$ ($x \leq 0.12$). Solid solutions $\text{CuMo}_{(1-x)}\text{W}_x\text{O}_4$ were synthesized within the domain of solubility of tungsten in CuMoO_4 ($0 \leq x \leq 0.12$) and the corresponding dense ceramics were obtained by spark plasma sintering.

EXPERIMENTAL PROCEDURES

The precursors were synthesized by the polymerizable complex method using the appropriate amounts of copper nitrate $\text{Cu}(\text{NO}_3)_2 \cdot 3\text{H}_2\text{O}$ (Acros organics, 99.9%), ammonium molybdate $(\text{NH}_4)_6\text{Mo}_7\text{O}_{24} \cdot 4\text{H}_2\text{O}$ (Sigma Aldrich, 99.8%), ammonium tungstate $(\text{NH}_4)_{10}\text{W}_{12}\text{O}_{41} \cdot 5\text{H}_2\text{O}$ (Acros organics, 99.0%) and citric acid (Acros organics, 99.9%). The synthesis procedure was similar to that used for the preparation of not doped α - CuMoO_4 [20]. The precursors obtained were calcined under air for 2 hours at 420 or 700°C depending on their tungsten content.

The ceramics were prepared using both conventional sintering in air performed in a muffle furnace and by spark plasma sintering (SPS). For conventional sintering, discs were formed by uniaxial pressing at 25 bars at room temperature in the presence of an organic binder (Rhodoviol) so as to avoid the phenomenon of rolling. The green density of the pellet is ~ 61% of theoretical density. Pellets were sintered at 520-700°C for 2 h in air with a heating rate of 2.5 °C/min. SPS was carried out using a Dr. Sinter 2080 device from Sumitomo Coal Mining (Fuji Electronic Industrial, Saitama, Japan). The same processing parameters were used for all the compositions. The

powder was placed in an 8 mm tungsten carbide die and then sintered at 300°C for 5 min under a pressure of 200MPa. The heating rate was set to 150°C/min.

The crystalline structure was investigated by X-ray diffraction analysis using a D4 Endeavor X-ray diffractometer ($\text{CuK}\alpha = 0.154056 \text{ nm}$ and $\text{CuK}\beta = 0.154044 \text{ nm}$, operating voltage 40 kV and current 40 mA). The grain size and morphology of the powders and the microstructure of the sintered ceramics were observed with a scanning electron microscope (SEM, JEOL JSM 6400). The sintering behavior was studied by dilatometry (TMA Setsys 16/18) under air flow (heating rat =2.5 °C/min).

RESULTS AND DISCUSSION

Powders

Fig.1-a shows the measured XRD data for the samples calcined under air at 420 for 2 hours. For $x \leq 0.075$, all diffraction peaks are attributable to a phase triclinic isostructural with $\alpha\text{-CuMoO}_4$ (JCPDS 073-0488). The XRD pattern shows no evidence of the presence of $\gamma\text{-CuMoO}_4$. For $0.075 < x \leq 0.12$, mixtures of three phases were identified: $\alpha\text{-CuMoO}_4$, $\gamma\text{-CuMoO}_4$ and CuWO_4 (JCPDS 088-0269). The calcination temperature had to be raised up to 700 °C to obtain a pure solid solutions isostructural with $\gamma\text{-CuMoO}_4$ (Fig.1-b).

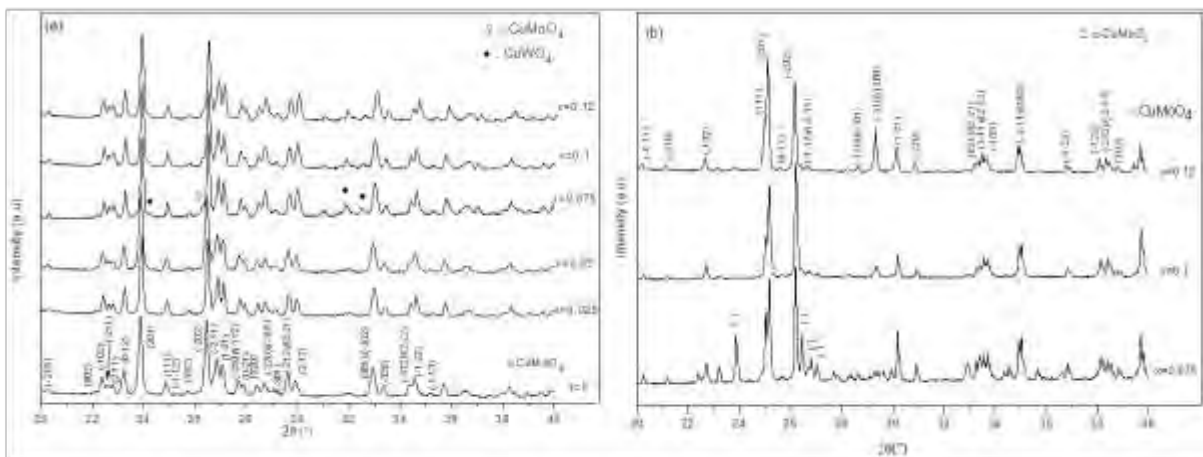


Fig.1. XRD patterns of $\text{CuMo}_{(1-x)}\text{W}_x\text{O}_4$ oxides after calcination of xerogels at (a) 420 and (b) 700°C for 2h. Miller indices are indicated for $\alpha\text{-CuMoO}_4$ (JCPDS 037-0488) and $\gamma\text{-CuMoO}_4$ (JCPDS 088-0620) phases.

The microstructures of solid solutions obtained by pyrolysis for 2h at 420 or 700°C were examined by scanning electron microscopy. The $\alpha\text{-CuMo}_{0.95}\text{W}_{0.05}\text{O}_4$ solid solution was constituted of particles agglomerated with a poly-disperse size distribution (Fig. 2-a). These agglomerates are consisted in elongated or more or less spherical elementary grains with sizes in the range 0.1-0.2 μm whereas the $\gamma\text{-CuMo}_{0.88}\text{W}_{0.12}\text{O}_4$ solid solution was constituted of relatively spherical grains with sizes included in the range 0.5-2.0 μm (Fig. 2-b).

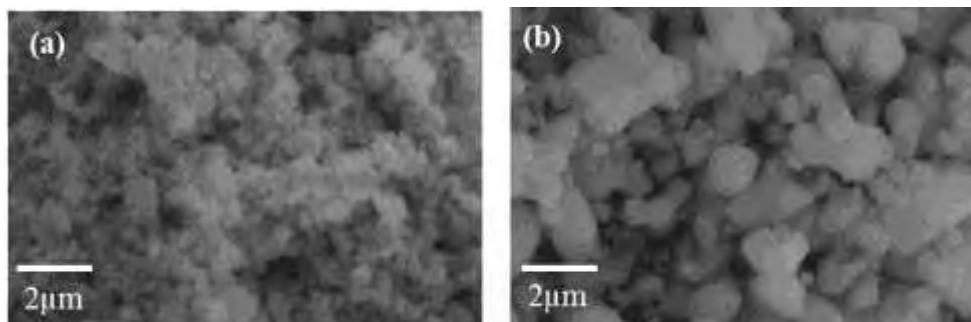


Fig.2. SEM micrographs of (a) $\alpha\text{-CuMo}_{0.95}\text{W}_{0.05}\text{O}_4$ and (b) $\gamma\text{-CuMo}_{0.88}\text{W}_{0.12}\text{O}_4$

Bulk ceramics

3.2a for $x \leq 0.05$

Fig. 3 shows the shrinking rates of the green compact $\alpha\text{-CuMo}_{(1-x)}\text{W}_x\text{O}_4$ ($x=0, 0.025$ and 0.05) powders via dilatometry under a constant heating rate of $2.5^\circ\text{C}/\text{min}$. As can be seen from Fig. 3, doping CuMoO_4 powders with W^{6+} cations delays the densification at higher temperatures. Indeed, the densification starts at ~ 470 and $\sim 505^\circ\text{C}$ for $x=0.025$ and $x=0.05$ respectively, compared $\sim 455^\circ\text{C}$ for pure CuMoO_4 . The higher densification rates of pure CuMoO_4 are obtained at 525°C , compared to 560 and 600°C for $x=0.025$, and $x=0.05$ respectively. The density of $\alpha\text{-CuMo}_{(1-x)}\text{W}_x\text{O}_4$ ($x \leq 0.05$) ceramics is determined to be $\sim 93\%$.

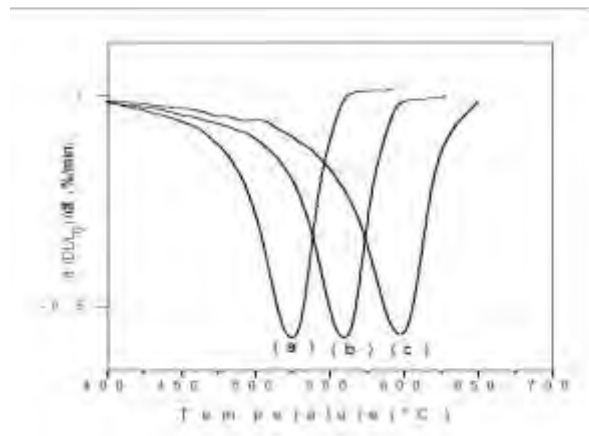


Fig.3. Shrinking rate versus temperature for $\text{CuMo}_{(1-x)}\text{W}_x\text{O}_4$ ceramics, (a) $x=0$, (b) $x=0.025$, (c) $x=0.050$

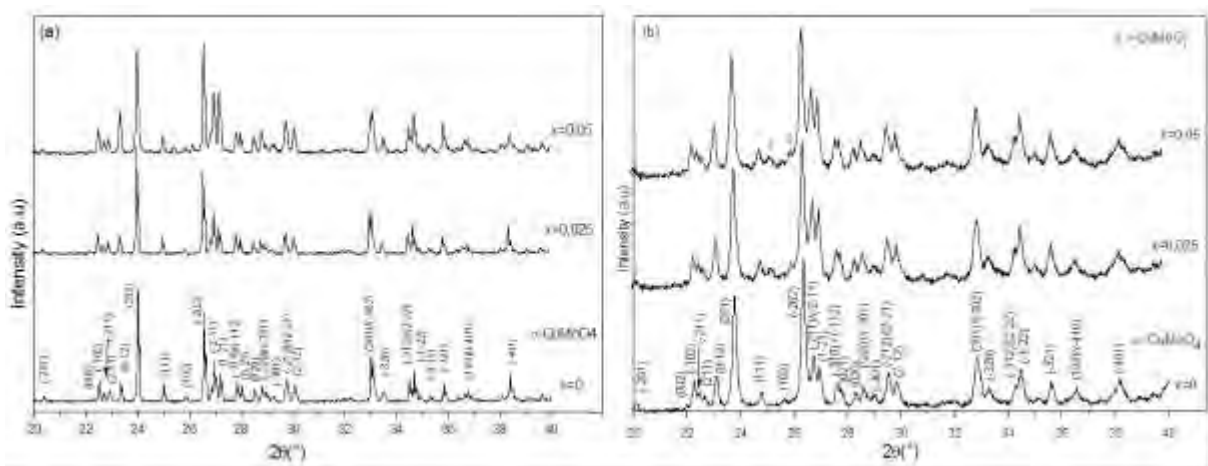


Fig.4. XRD patterns of $\text{CuMo}_{(1-x)}\text{W}_x\text{O}_4$ ($x=0, 0.025$ and 0.05): (a) conventionally sintered and (b) SPS sintered at 300°C for 5 min with an applied pressure of 200 MPa. Miller indices are indicated for a (JCPDS 037-0488) phase.

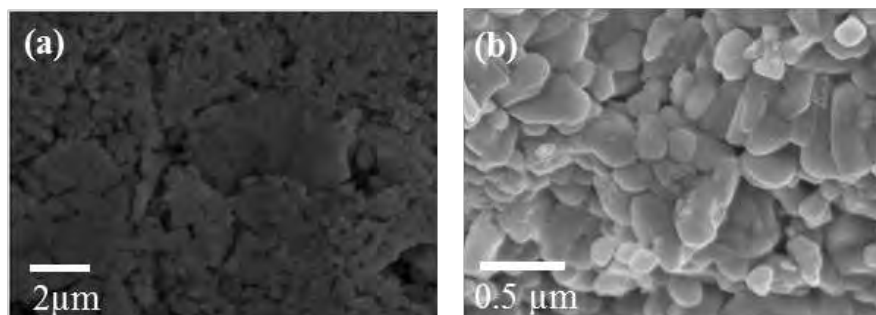


Fig.5. SEM micrographs of $\text{CuMo}_{0.95}\text{W}_{0.05}\text{O}_4$: (a) conventionally sintered at 600°C for 2 h, and (b) SPS sintered at 300°C for 5 min with an applied pressure of 200 MPa

The XRD patterns of the ceramics sintered by SPS at 300°C for 5 min under a pressure of 200 MPa showed, for $x=0.025$ and $x=0.05$, that the molybdate γ -CuMoO₄ was formed beside α -CuMoO₄ whereas those conventionally sintered are not modified by the thermal treatment (Fig.4).

The microstructures of the CuMo_{0.095}W_{0.05}O₄ ceramics prepared by the conventional sintering at 600°C for 2h and by spark plasma sintering (SPS) at 300°C for 5min with an applied pressure of 200MPa were examined by SEM. As shown in Fig. 5a, large pores were observed both at the grain boundaries and within the agglomerates in the conventionally sintered ceramics, indicating that the specimen was not really dense. For SPS samples (Fig. 5b), the grain sizes did not exceed 200 nm, with a relatively narrow granulometric distribution. Little residual porosity was observed. The broadness of the X-ray diffraction peaks of SPS sintered ceramic was comparable to that of the peaks of the non-sintered powder whereas the peaks of the conventionally sintered ceramic were significantly narrower (Fig.4). The SEM micrographs (Fig.5) are confirmed, i.e. on the contrary of conventional route, the SPS allows the limitation of the grain growth.

3.2b for $0.075 < x \leq 0.12$

In order to better understand the sintering behavior of γ -CuMo_(1-x)W_xO₄ ($0.075 < x \leq 0.12$) powders, dilatometry experiments was performed on the γ -CuMo_{0.88}W_{0.12}O₄ powder (Fig. 6). The dilatometric curve is characteristic of a sintering process in several stages. The shrinkage starts around 450 °C and ends after about two hour at 700 °C

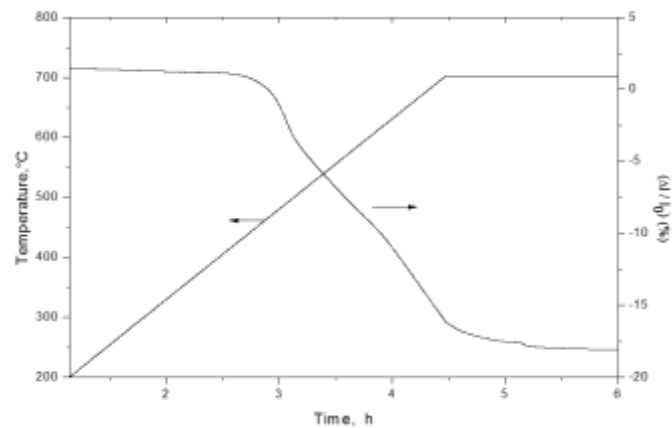


Fig. 6. Dilatometric behavior of CuMo_{0.88}W_{0.12}O₄

The ceramics obtained after sintering at 700°C for 2 hours and by SPS at 300° C for 5 min under a pressure of 200MPa were characterized by X-ray diffraction analysis (Fig.7) and by SEM (Fig. 8). All the peaks of X-ray diffraction patterns of CuMo_(1-x)W_xO₄ ($0.075 < x \leq 0.12$) were indexed in a triclinic lattice with the space group $P\bar{1}$, whatever the sintering procedure (Fig.7). The polymorphic form was dependent upon the sintering procedure. For conventional sintering, the solid solutions were isostructural with α -CuMoO₄ whereas for SPS they were isostructural with CuMoO₄-III (JCPDS 077-0699). In both cases, γ -CuMoO₄ appeared as minor structure.

The ceramics conventionally sintered at 700 °C for 2h were consisted of grains sized in the range 1-5 μ m and abnormal growth of some grains are observed (Fig. 8a). The sample sintered by SPS at 300°C for 5min presents much denser microstructure with largely grown platelets (Fig. 8b).

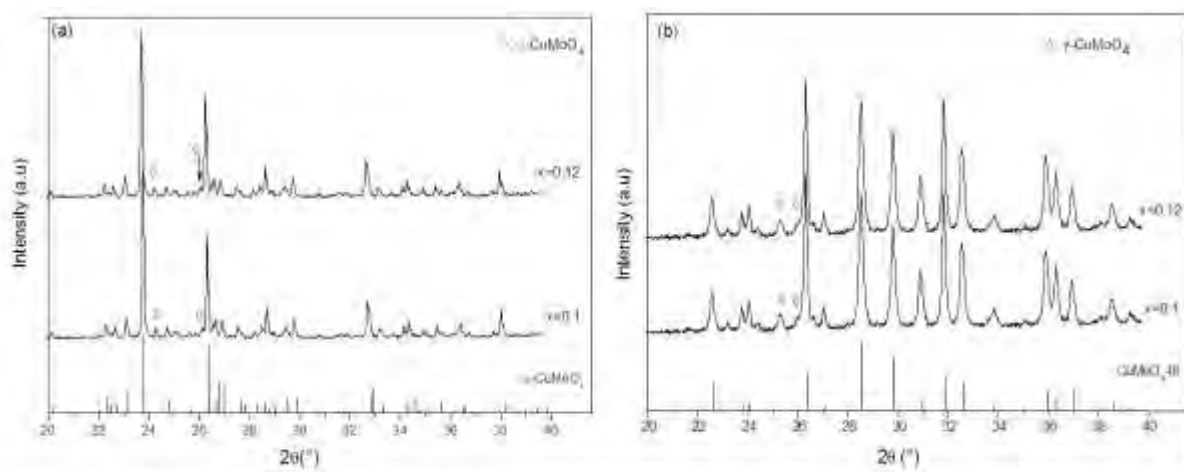


Fig.7. XRD patterns of $\text{CuMo}_{(1-x)}\text{W}_x\text{O}_4$ (with $x=0.1$ and 0.12): (a) conventionally sintered at $700\text{ }^\circ\text{C}$ for 2 h, and (b) SPS sintered at $300\text{ }^\circ\text{C}$ for 5 min with an applied pressure of 200 MPa.

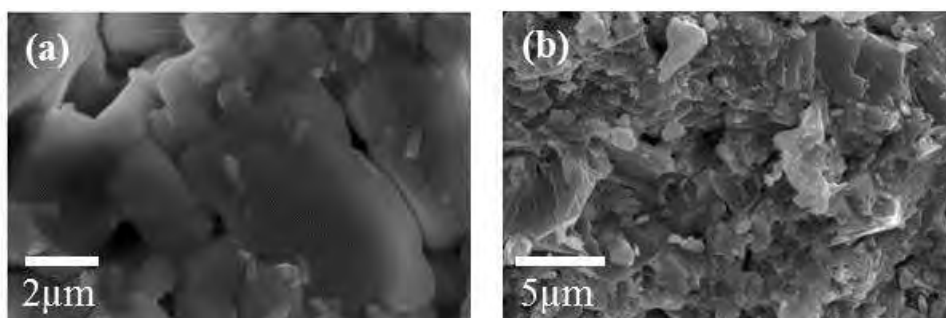


Fig.8. SEM micrographs of $\text{CuMo}_{0.88}\text{W}_{0.12}\text{O}_4$: (a) conventionally sintered at $700\text{ }^\circ\text{C}$ for 2 h, and (b) SPS sintered at $300\text{ }^\circ\text{C}$ for 5 min with an applied pressure of 200 MPa

CONCLUSION

W-substituted CuMoO_4 compounds, $\text{CuMo}_{(1-x)}\text{W}_x\text{O}_4$ ($0 \leq x \leq 0.12$), were obtained by pyrolysis at temperature in the range $420\text{--}700\text{ }^\circ\text{C}$ for 2 hours of a gels prepared by the polymerizable complex method. For $x \leq 0.075$, they were isostructural to $\alpha\text{-CuMoO}_4$ whereas, for $0.075 < x \leq 0.12$, they were isostructural to $\gamma\text{-CuMoO}_4$. Spark plasma sintering at $300\text{ }^\circ\text{C}$ for 5 min under a pressure of 200 MPa led to variety $\text{CuMoO}_4\text{-III}$ for tungsten contents in the range $0.075\text{--}0.12$.

ACKNOWLEDGMENTS

This work was supported by two French-Moroccan projects: Volubilis Partenariat Hubert Curien (PHC no. MA 09 205) and Projet de Recherches Convention Internationale du CNRS (CNRS-CNRST no w22572).

REFERENCES

1. L.A. Palacio, A.Echavarri, L. Sierra and E. A. Lombardo, "Cu, Mn and Co molybdates derived from novel precursors catalyze the oxidative dehydrogenation of propane," in *catal. Today*, vol.107-108, pp.338-345, 2005.
2. N.V. Lebukhova, V.S. Rudnev, P.G. Chigrin, I.V. Lukiyanchuk, M.A. Pugachevsky, A.J. Ustinov, E.A. Kirichenko, and T.P. Yarovaya, "The nanostructural catalytic composition $\text{CuMoO}_4/\text{TiO}_2+\text{SiO}_2/\text{Ti}$ for combustion of diesel soot," in *Surf. Coat.Tech.*, vol. 231, pp. 144-148,2013.
3. M.D. Ward, J.F. Brazdil, S.P. Mehandru and A.B. Anderson, "Methane photoactivation on copper molybdate: an experimental and theoretical study," in *J. Phys. Chem.*, vol.91, pp. 6515- 6521,1987.
4. I. Yanasen, T. Mizuno and H. Kobayashi, "Structural phase transition and thermochromics behavior of synthesized W substituted CuMoO_4 ," in *Ceram. Int.*, vol.39, issue 2, pp. 2059-2064, 2013.

5. H. J. Koo and M.H. Whangbo, "Spin Dimer Analysis of the Anisotropic Spin Exchange Interactions in the Distorted Wolframite-Type Oxides CuWO_4 , CuMoO_4 -III, and $\text{Cu}(\text{Mo}_{0.25}\text{W}_{0.75})\text{O}_4$," in *Inorg. Chem.*, vol. 40, issue 9, pp. 2161-2169, 2001.
6. B.C. Schwarz, H. Ehrenberg, H. Weitzel and H. Fuess, "Investigation on the influence of particular structure parameters on the anisotropic spin-exchange interactions in the distorted Wolframite-type oxides $\text{Cu}(\text{MoxW}_{1-x})\text{O}_4$," in *Inorg. Chem.*, vol. 46, pp. 378-380, 2007.
7. M. Wiesmann, H. Ehrenberg, G. Miehe, T. Peun, H. Weitzel and H. Fuess, "p-T Phase Diagram of CuMoO_4 ," in *J. Solid State Chem.*, vol. 132, issue 1, pp. 88-97, 1997.
8. G. Mul, J.P.A. Neeft, F. Kapteijn, M. Makkee and J.A. Moulijn, "Soot oxidation catalyzed by a Cu/K/Mo/Cl catalyst: evaluation of the chemistry and performance of the catalyst," in *Appl. Catal. B*, vol. 6, issue 4, pp. 339-352, 1995.
9. J. Haber, T. Machej, L. Ungier and J. Ziolkowski, "ESCA studies of copper oxides and copper molybdates," in *J. Solid State Chem.*, vol. 25, pp. 207-218, 1978.
10. G. Steiner, R. Salzer and W. Reichelt, "Temperature dependence of the optical properties of CuMoO_4 ," in *Fresenius J. Anal. Chem.*, vol. 370, pp. 731-734, 2001.
11. M. Benchikhi, R. El Ouatib, L. Er-Rakho, S. Guillemet Fritsch, B. Durand, F. Olivie and K. Kassmi, "Morphological and electric characterizations of a nanometric material α - CuMoO_4 for photovoltaic application," in *J. Mater. Environ. Sci.*, vol. 4, issue 2, pp. 504-509, 2013.
12. J. Baek, A.S. Sefat, D. Mandrus and P. Shiv Halasyamani, "A New Magnetically Ordered Polymorph of CuMoO_4 : Synthesis and Characterization of ϵ - CuMoO_4 ," in *Chem. Mater.*, vol. 20, issue 12, pp. 3785-3787, 2008.
13. H. Ehrenberg, H. Weitzel, H. Paulus, M. Wiesmann, G. Wltschek, M. Geselle and H. Fuess H., "crystal structure and magnetic properties of CuMoO_4 at low temperature (γ -phase)," in *J. Phys. Chem.*, vol. 58, issue 1, pp. 153-160, 1997.
14. A. W. Sleight, "High pressure CuMoO_4 ," in *Mater. Res. Bull.*, vol. 8, pp. 863-866, 1973.
15. H. Ehrenberg, M. Wiesmann, J. Garcia-Jaca, H. Weitzel and H. Fuess, "Magnetic structures of the high-pressure modifications of CoMoO_4 and CuMoO_4 ," in *J. Magn. Magn. Mater.*, vol. 182, pp. 292-303, 1998.
16. D. Klissurski, R. Iordanova, M. Milanova, D. Radev and S. Vassilev, "Mechanochemically Assisted Synthesis of Cu (II) Molybdate," in *CR Acad. Bulgare Sci.*, vol. 56, pp. 39-42, 2003.
17. S. Mitchell, A. Gomez Aviles, C. Gardner and W. Jones, "Comparative study of the synthesis of layered transition metal molybdates," in *J. Solid State Chem.*, vol. 183, pp. 198-207, 2010.
18. K.S. Makarevich, N.V. Lebukhova, P.G. Chigrin and N.F. Karpovich, "Catalytic Properties of CuMoO_4 Doped with Co, Ni, and Ag," in *Inorg. Mater.*, vol. 46, issue 12, pp. 1494-1499, 2010.
19. P. Schmitt, N. Brem, S. Schunk and C. Feldmann, "Polyol-Mediated Synthesis and Properties of Nanoscale Molybdates/Tungstates: Color, Luminescence, Catalysis," in *Adv. Funct. Mater.*, vol. 21, issue 16, pp. 3037-3046, 2011.
20. M. Benchikhi, R. El Ouatib, S. Guillemet Fritsch, J.Y. Chane Ching, L. Er-rakho and B. Durand, "Sol-gel synthesis and sintering of submicronic copper molybdate (α - CuMoO_4) powders," in *Ceram. Int.*, vol. 40, issue 4, pp. 5371-5377, 2014.
21. M. Benchikhi, R. El Ouatib, L. Er-Rakho, S. Guillemet Fritsch, B. Durand and K. Kassmi, "Influence of chelating agent on the morphological properties of α - CuMoO_4 powder synthesized by sol-gel method," in *J. Mater. Environ. Sci.*, vol. 6, issue 12, pp. 3470-3475, 2015.
22. S.M. Montemayor, L.A. García Cerda and J.R. Torres-Lubián, "Preparation and characterization of cobalt ferrite by the polymerized complex method," in *Mater. Lett.*, vol. 59, issues 8-9, pp. 1056-1060, 2005.
23. H. Lakhlifi, M. Benchikhi, R. El Ouatib, L. Er-Rakho, S. Guillemet Fritsch and B. Durand, "Synthesis and physicochemical characterization of pigments based on molybdenum « $\text{ZnO-MoO}_3: \text{Co}^{2+}$ », " in *J. Mater. Environ. Sci.*, vol. 6, issue 12, pp. 3465-3469, 2015.